Clim Dyn
DOI 10.1007/s00382-014-2464-2

Impact of aerosol radiative effects on 2000–2010 surface temperatures

A. Gettelman · D. T. Shindell · J. F. Lamarque

Received: 15 September 2014 / Accepted: 25 December 2014

Abstract Aerosol radiative forcing from direct and indirect effects of aerosols is examined over the recent past (last 10–15 years) using updated sulfate aerosol emissions in two Earth System Models with very different surface temperature responses to aerosol forcing. The hypothesis is that aerosol forcing and in particular, the impact of indirect effects of aerosols on clouds (Aerosol–Cloud Interactions, or ACI), explains the recent 'hiatus' in global mean surface temperature increases. Sulfate aerosol emissions increase globally from 2000 to 2005, and then decrease slightly to 2010. Thus the change in anthropogenic sulfate induced net global radiative forcing is small over the period. Regionally, there are statistically significant forcings that are similar in both models, and consistent with changes in simulated emissions and aerosol optical depth. Coupled model simulations are performed to look at impacts of the forcing on recent surface temperatures. Temperature response patterns in the models are similar, and reflect the regional radiative forcing. Pattern correlations indicate significant correlations between observed decadal surface temperature changes and simulated surface temperature changes from recent sulfate aerosol forcing in an equilibrium framework. Sulfate ACI might be a contributor to the spatial patterns of recent temperature forcing, but not to the global mean 'hiatus' itself.

Keywords Climate · Aerosol · Forcing

A. Gettelman (✉) · J. F. Lamarque
National Center for Atmospheric Research, Boulder, CO, USA
e-mail: andrew@ucar.edu

D. T. Shindell
Nicholas School of the Environment, Duke University, Durham, NC, USA

1 Introduction

Aerosol particles have significant direct cooling effects by scattering sunlight. Aerosols also have significant 'indirect' effects on the planetary energy balance by modifying cloud properties and distributions, termed aerosol cloud interactions (ACI). These effects were recently reviewed by Boucher et al. (2013). The net effect of ACI due to anthropogenic aerosols is a cooling due to the brightening of clouds resulting from higher cloud drop number concentrations induced by higher cloud condensation nuclei (CCN) concentrations (Twomey 1977) and from clouds with smaller drops precipitating less and having a longer lifetime and increased cloud liquid water content (Albrecht 1989). Aerosol indirect radiative effects are uncertain, and estimated to be -0.9 (-0.1 to -1.9) Wm^{-2} (cooling) with the present day (year 2000) emissions of anthropogenic aerosols (Boucher et al. 2013).

But anthropogenic aerosol emissions have changed over the last few decades. Global emissions peaked in the 1970s (Lamarque et al. 2010) before air pollution regulations were enacted in developed countries, mostly in N. America and W. Europe. Now global aerosol emissions are rising once again due to increases in developing economies (Klimont et al. 2013). The growth has been particularly rapid in the last 10–15 years, especially with the growth of emissions in China. Recent changes in SO_2 (the anthropogenic emission with the largest effects on liquid clouds) beyond 2000 have been estimated by Klimont et al. (2013). Increases in global emissions are estimated between 2000 and 2005, with decreases from 2005 to 2010. The decrease is consistent with air pollution controls instituted in China in 2006 (Lu et al. 2010). There are large decreases in N. America and Europe over the first decade of the twentyfirst century.

Published online: 06 January 2015

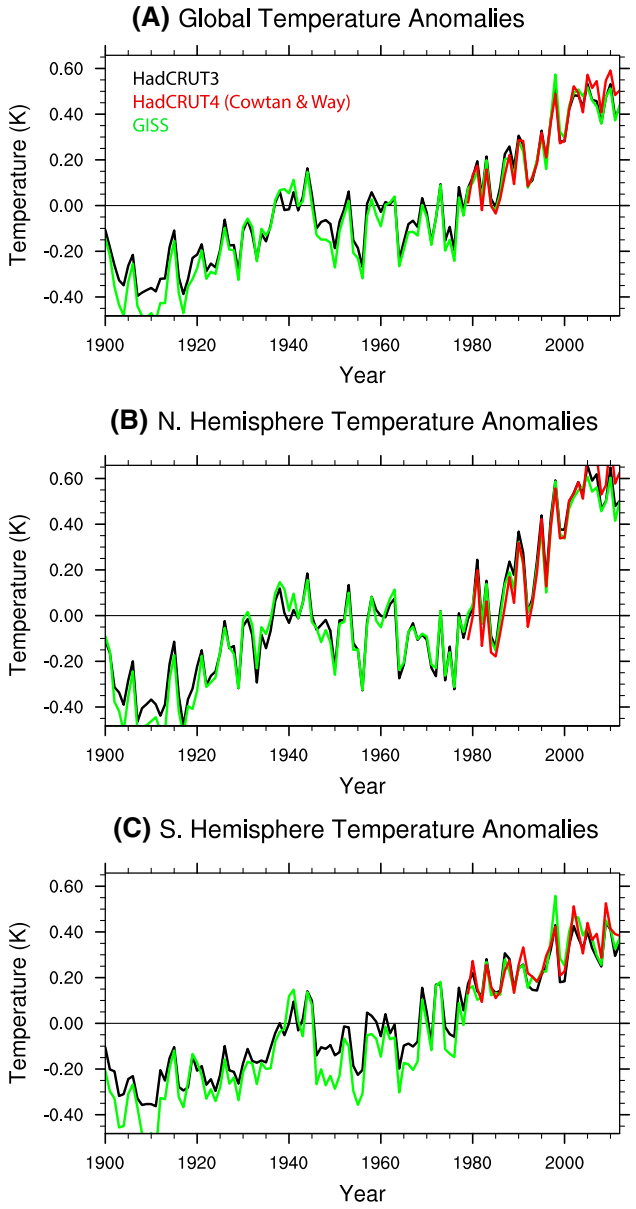

Fig. 1 **a** Global, **b** N. Hemisphere and **c** S. Hemisphere annual temperature anomalies from the 1900 to 2012 average. HadCRUT3 (*black*), HadCRUT4 from Cowtan and Way (2014) (*red*) and GISS (*green*) lines

Coincident with the increasing aerosol emissions, global average temperature has not risen much over the last 15 years (Hartmann et al. 2013). This 'hiatus' period comes in the midst of a century-long global average warming trend (Hartmann et al. 2013). Figure 1 illustrates clearly that this is just a small blip on an much longer record. Three different analyses of the surface temperature record are presented: (1) HadCRUT3 data (black line in Fig. 1) from the Hadley Centre and Climatic Research Unit (Brohan et al. 2006), (2) HadCRUT4 data from Cowtan and Way (2014) (red line in Fig. 1) and (3) NASA Goddard Institute for Space Studies (GISS) data (green line in Fig. 1) described by Hansen et al. (2010). The choice of data source does not change the qualitative message: the planet has not warmed much globally since 1998 (largely due to a large El Nino event that year). A look by hemisphere indicates that this is mostly a feature of the N. Hemisphere, which has actually slightly cooled over the period since 2005, while the S. Hemisphere trends are more monotonic. Similar results are presented by Hartmann et al. (2013). Note that Cowtan and Way (2014) data correct for an Arctic sampling bias and this does reduce the apparent hiatus, which is not apparent in global mean temperature if the bias is removed.

Many authors have looked at what might cause a 15 year 'pause' in the long term warming trend. As there are many possible explanations, the problem is 'overdetermined'. Possible causes of a 'hiatus' in global mean surface temperature include: unforced variability in the system Kaufmann et al. (2011) due to increases in ocean heat uptake (Trenberth et al. 2014; Chen and Tung 2014), changes in stratospheric water vapor (Solomon et al. 2010), changes in the solar cycle (Lean and Rind 2009), ocean variability in the tropical Pacific (Kosaka and Xie 2013) or changes in aerosol forcing. The latter can be broken down into changes due to an increase in stratospheric reflective sulfur aerosols due to volcanic activity (Solomon et al. 2011) or changes to the direct and indirect effect of anthropogenic aerosols in the troposphere (Booth et al. 2012; Schmidt et al. 2014a).

The magnitude of these effects can also be estimated and was recently assessed by Schmidt et al. (2014a). The total radiative forcing from well mixed anthropogenic greenhouse gases has changed by about $+0.35\ \mathrm{Wm}^{-2}$ between 2000 and 2010, estimated from concentration changes observed by the the NOAA Global Monitoring Division flask sampling network. The estimated change in ocean heat uptake is about $-0.21\,\mathrm{Wm}^{-2}$ over the last decade (Trenberth et al. 2014). Stratospheric water vapor changes might account for $-0.1\,\mathrm{Wm}^{-2}$ (Solomon et al. 2010), and forcing due to recent volcanic activity for another $-0.1\,\mathrm{Wm}^{-2}$ (Solomon et al. 2011). Aerosol effects (ACI) were estimated by Schmidt et al. (2014a) to be an additional $-0.1\,\mathrm{Wm}^{-2}$, but they assumed ACI followed NO_2 (not SO_2) emissions, without direct simulations.

In this work we explore the hypothesis that the direct and indirect effects of recent increases in aerosols, mostly from anthropogenic SO_2, are a detectable part of the anthropogenic radiative forcing and temperature trends over the last 10–15 years. The hypothesis comes from the observation that aerosol emissions have increased over the last 15 years in some regions of the planet, mostly in the N. Hemisphere, and that the temperature trends (Fig. 1) ascribe most of the

hiatus to the N. Hemisphere. The hypothesis is tested using adjusted aerosol emissions data sets, and two state of the art Earth System Models that can simulate ACI, the resulting radiative forcing, and its effect on surface temperature. We conclude with a simple but equivocal result: the global magnitude of the aerosol effect between 2000 and 2010 is not significantly different from zero because of a change of sign of global SO_2 emission trends over the period. But there are significant regional changes to simulated forcing and temperature response patterns that are similar to observed changes.

Section 2 describes the methodology. Results are in Sect. 3 and conclusions are in Sect. 4.

2 Methodology

2.1 Model descriptions

We use two global earth system models for this study. One is the Community Earth System Model (CESM), (Hurrell et al. 2013). The version we use contains version 5 of the Community Atmosphere Model [CAM5, Neale et al. (2010)]. CAM5 contains a detailed treatment of cloud microphysics and aerosol effects by linking a 2-mode bulk microphysics scheme (Morrison and Gettelman 2008) to a 3-mode modal aerosol model (MAM3) (Liu 2012) with detailed descriptions of droplet activation and ice nucleation of cloud drops on aerosols (Gettelman et al. 2010). MAM3 simulates internal mixtures of dust, sea-salt, sulfate, organics and black carbon. The model simulates both direct and indirect effects of aerosols, the latter now referred to as ACI. This model is the equivalent to the CESM1–CAM5 configuration used in the Coupled Model Intercomparison Project (CMIP) phase 5 (Taylor et al. 2012).

The other model is the NASA GISS ModelE2-R (hereafter ModelE2) (Schmidt et al. 2014b). ModelE2 contains a mass-based aerosol model under which sulfate, carbonaceous and nitrate aerosols are considered externally mixed and have prescribed properties and sizes (Koch et al. 2007). Natural sea-salt and mineral dust aerosols have two and four size bins, respectively. The version of the model used here is a coupled ocean-atmosphere model as used in the GISS ModelE2-R physics version 3 simulations for CMIP5. For aerosol-cloud interactions, only the so-called cloud albedo (first indirect) effect is included using a prognostic treatment of CDNC from Morrison and Gettelman (2008) as a function of sources, including newly nucleated CDNC and losses from autoconversion, contact nucleation, and via immersion freezing (Menon et al. 2010). Aerosol effects do not feed back on autoconversion and cloud lifetime in this version of ModelE2. The microphysics do not see variable drop numbers. See Schmidt et al. (2014b) for details.

2.2 Simulations

Two types of radiative flux perturbation experiments are performed with CESM. These experiments are designed to isolate the effect of relatively small perturbations of aerosol emissions on climate. First, we use atmosphere only simulations with fixed greenhouse gases (GHGs), sea surface temperatures (SSTs) and fixed meteorology (Lamarque et al. 2012) to derive the radiative forcing from anthropogenic aerosol emissions. Note that in all CESM simulations, GHGs are fixed at year 2000 levels and are not an additional forcing. Fixed meteorology, or specified dynamics (SD) simulations are performed by taking winds and temperatures from a previous run with 2006 SST, GHG and aerosol forcing and specifying these fields as input to the dynamical core. The use of specified dynamics constrains winds and temperatures, but allows the model to prognose and advect aerosols, humidity and clouds. The interactions are treated consistently, but meteorological noise and variability is eliminated. This increases the signal to noise ratio for small forcing perturbations. SD simulations are run for 12 years, with the last 10 years analyzed (repeating the same conditions each year). We compare SD runs with 2006 SSTs with a free running model run for 50 years with climatological SSTs representing 1980–2000 averages, just to illustrate that results are not sensitive to the SD method of estimating forcing.

Second, we use CESM configured with a slab (or mixed layer) ocean model to explore the effect of the radiative perturbations on sea surface temperatures. Instead of specified boundary conditions, the surface conditions are determined by assuming the ocean is a single layer under each column of spatially variable depth, with a specified heat flux to or from the deep ocean (Bitz et al. 2012). These simulations do not have specified dynamics. Slab ocean experiments have the advantage over a coupled ocean in that they can easily be run to equilibrium. Simulations take about 20 years for surface temperatures to adjust, and then they are run for 60 more years to average out internal variability. CESM Slab ocean simulations are 80 years, with the last 50 years analyzed. All CESM simulations are at 1.9° latitude by 2.5° longitude resolution with 30 levels from the surface to 2 hPa. CESM simulations use a constant annual cycle of emissions in each simulation (emissions vary between simulations).

ModelE2 simulations are set up slightly differently. Simulations to diagnose the radiative forcing due to aerosol emissions were run using fixed-SSTs, as in the CESM case, but with internally generated meteorology, similar to the free running CESM case. Fixed-SSTs are from ensemble mean averages of the decade 2000–2010 from ModelE2 CMIP5 simulations. Given the larger inherent variability, these simulations were extended for 100 years,

with the analysis presented here covering the last 90 years of the simulations. As in CESM, a constant annual cycle of emissions is used in each simulation. In these simulations, temperature can respond to aerosols, so these simulations (and the slab ocean CESM simulations) include the 'semi-direct' effect of aerosol absorption, which the SD simulations do not. Surface temperature responses to aerosol forcing are taken from simulations run with the coupled-ocean atmosphere version ModelE2-R following GISS historical CMIP5 simulations (Miller et al. 2014) in all respects except being driven by tropospheric (i.e. excluding large volcanic eruptions) aerosol forcing alone. Decadal time periods (11 years centered on the nominal analysis year) are analyzed drawing output from five ensemble members to provide 55 years of model output except for the 2010 time period that includes 2008–2012 (the end of the historical simulations) and hence contains only 25 years. All ModelE2 simulations were at 2° latitude by 2.5° longitude with 40 vertical layers from the surface to 0.1 hPa.

The goal of coupled simulations is to compare simulated 'equilibrium' responses to aerosol forcing alone with the observed temperature record. Model responses give us hypotheses of the effect of aerosol changes, and we can test the response (temperature change) against the observed temperature change. The real system includes transients (internal variability) and multiple forcings that complicate 'fingerprinting' the cause of the response. We will compare the observed temperature response to the simulated 'equilibrium' single forcing response to see if there is a significant correlation.

We are using two different coupling methods to try to dis-entangle the effect of a small forcing observed in the coupled system. One is the slab (mixed layer) ocean configuration in CESM. The other is a small ensemble of single forcing coupled simulations from ModelE2 with a full ocean model. We are seeking an 'equilibrium' response to the perturbed aerosol forcing. An ensemble of coupled simulations is one option. The slab ocean is another method. The difficulty of transient simulations is that for a small forcing perturbation on the order of 0.1 Wm^{-2}, variability in the coupled system, particularly the ocean heat uptake will swamp the forcing, even for long simulations. A slab ocean reduces this degree of freedom by fixing the deep ocean heat flux. The CESM slab ocean model is described by Bitz et al. (2012) and was found to reproduce the impact of forcing in the fully coupled CESM simulation. In a more detailed investigation of slab ocean models, Shell (2013) found that feedbacks are similar between slab ocean and coupled simulations, with slightly lower water vapor and lapse rate feedbacks in slab ocean simulations, as a result of coupling with deep ocean heat transport. But for small perturbations discussed here, that should not be an issue. Nevertheless, part of the motivation of the multi-model study was to look at the available coupled and slab simulations in different ways, and we show below that the basic conclusions can be seen in different models with different coupling strategies.

2.3 Emissions

Baseline aerosol emissions are from Lamarque et al. (2010) for the historical period up to 2005. The CMIP5 simulations were performed with Representative Concentration Pathways (RCPs) for aerosol and greenhouse gas emissions after 2005. Klimont et al. (2013) have estimated updates in SO_2 emissions since 2005. SO_2 rapidly becomes a CCN and is a significant contributor to ACI (e.g. Boucher et al. 2013, FAQ 7.2). This is also true specifically in CESM1–CAM5 (Gettelman et al. 2010), so we focus on perturbations to SO_2 emissions.

In order to be consistent with emissions used in Lamarque et al. (2010), and therefore CMIP5 simulations, we take the difference in annual gridded emissions at each point between 2000 and 2010 estimated by Klimont et al. (2013) and apply it to each emissions sector in 2000. This provides a consistent treatment with the Lamarque et al. (2010) emissions used in CESM and Model E2. For points over the ocean, the only active emissions sector is ship emissions. Klimont et al. (2013) report only an annual global total increase from 9.8 to 13.6 $TgSO_2$ (Klimont et al. (2013), Table S-1), so we uniformly scale international shipping emissions of SO_2 by this ratio (+39 %). Emissions are regridded from 0.5° to model input resolution. The same emissions are used in both CESM and ModelE2.

Figure 2 illustrates the different emissions of SO_2 as percent changes. Klimont et al. (2013) report increases in emissions in Asia and Africa between 2000 and 2005, while there are decreases in the Americas and Europe (Fig. 2a). Between 2000 and 2010, there are large increases in E and S. E. Asia, and parts of sub-Saharan Africa, with decreases in N. America, Europe and Russia (Fig. 2b). Note that many of these areas (like Tibet, or Zambia) have low emissions to begin with, so the large percent changes do not matter globally. The corresponding change in RCP emissions used in the CMIP5 experiments (Fig. 2c) is different, with smaller changes in N. America, Europe and Russia, and larger changes in Africa, along with slightly different baseline ship emissions. RCP emissions projected decreases in ship emissions of 2–4 % between 2000 and 2010. The 2010 scaled RCP emissions (scaled using the differences in percent in Fig. 2b) are in Fig. 2d, they are regridded, but otherwise very similar. We have also explored several different methods of scaling emissions: (1) uniform scaling by total emissions as stated above as the base case, (2) by sector termed 'A', and (3) with limits on the ratios of 2010–2000 emissions, 'A2'. Results are quantitatively similar with all different methods: the results are not very sensitive to the choice of method.

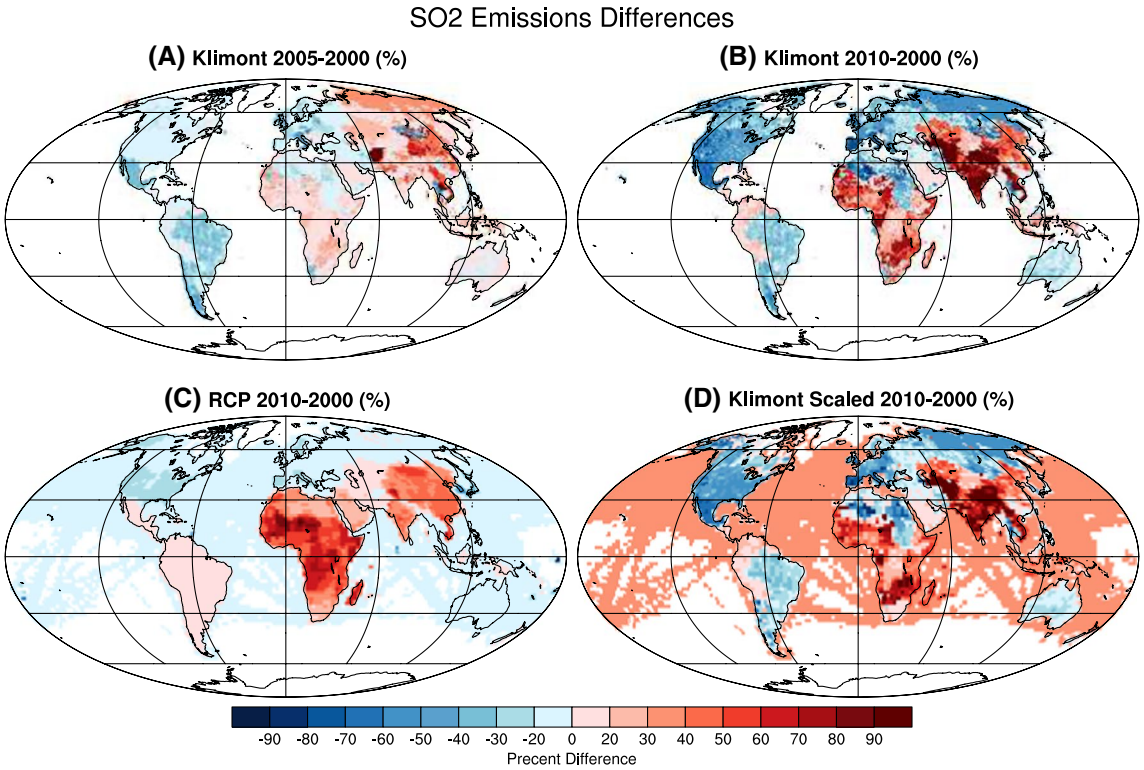

Fig. 2 Differences in annual surface SO_2 emissions (in percent). **a** 2005–2000 from Klimont et al. (2013) estimates. **b** 2010–2000 from Klimont et al. (2013). **c** 2010–2000 from RCP4.5. **d** Take 2000 IPCC emissions and scale based on 2010–2000 Klimont, by sectors, with increased shipping emissions

3 Results

3.1 Radiative forcing

For forcing, we examine focused experiments with aerosol emissions for 1850, 1980 and 2010 relative to the year 2000.

Specified dynamics (SD) runs are used to determine radiative forcing with CESM. Figure 3 illustrates an example, using SD simulations with 2000 aerosol emissions, and 1850 (pre-industrial) emissions. There are significant increases in visible aerosol optical depth (AOD or AEROD: Fig. 3a) thoroughout the N. Hemisphere, with largest changes in E. Asia. Note that these emissions are more than just increases in SO_2 but also represent changes in organic and inorganic carbon, interactive dust and secondary organic aerosols. The resulting change in top of atmosphere (TOA) radiative flux is illustrated in Fig. 3b. Negative forcing (cooling) occurs in the Pacific sector. There is less change in aerosols and TOA forcing over N. America and Europe. The direct effects of aerosol scattering and absorption can be estimated by a diagnostic call to the radiation code with no aerosols, and a difference between these fluxes (Fig. 3c). The net direct effects are small. The majority of the TOA changes are due to ACI or indirect effects of aerosols altering cloud radiative effects (CRE) illustrated as the sum of long wave and short wave effects in Fig. 3d. The ACI can also be estimated as the residual of the total TOA change and the direct effect. This value is very similar to the CRE change. Note that for SD simulations, the two standard deviation (2σ, 95 % significance) level for annual mean TOA fluxes at any point using a 10 year simulation is about 0.4–0.5 Wm^{-2} (lower at the poles, higher at the equator), so these differences are all highly significant.

Figure 4 illustrates the change in forcing between 2000 and 1850 from ModelE2. The patterns of change are similar to CESM (Fig. 3), but note that the contour intervals are different: AOD changes are larger in ModelE2, but the peak forcing changes are smaller by a factor of two than CESM (Fig. 3). The regions are more extensive though, and the global total forcing is comparable.

The quantitative global values for CESM SD simulations, ModelE2 free running simulations and a free running CESM simulation are illustrated in Table 1. For Fig. 3, CESM 2000–1850, the total change in TOA flux (dF) is $-1.42\,\mathrm{Wm}^{-2}$, with ACI representing $-1.21\,\mathrm{Wm}^{-2}$ (ΔCRE). The corresponding direct effects are $-0.07\,\mathrm{Wm}^{-2}$ using a dual call to the radiation code with and without aerosols. Ghan (2013) has recently proposed a slightly different framework for these calculations, removing the impact of

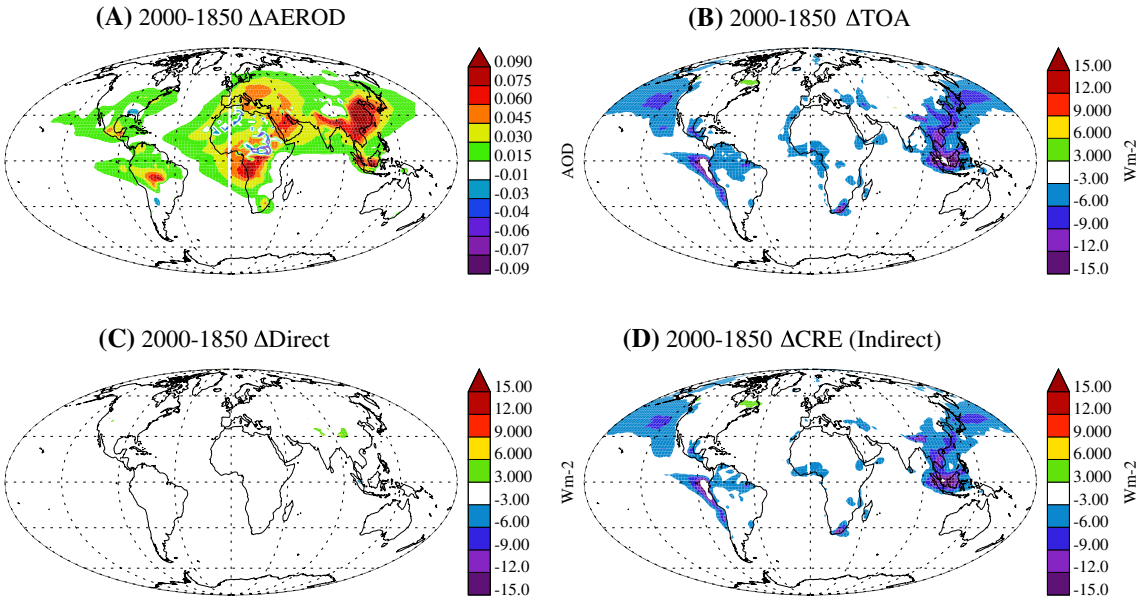

Fig. 3 Radiative forcing from CESM specified dynamics simulations based on 2000–1850 emissions. **a** Change in aerosol optical depth (AEROD), **b** change in top of atmosphere (TOA) radiation, **c** direct effect of aerosols, **d** change in cloud radiative effect (CRE) or indirect effect of aerosols

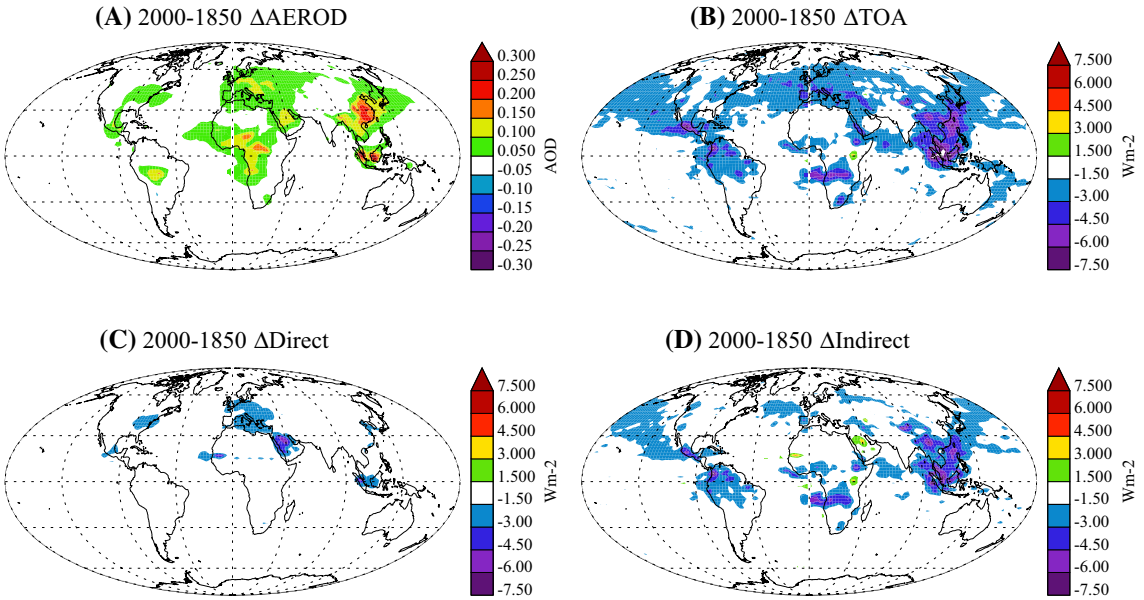

Fig. 4 Radiative forcing from ModelE2 simulations based on 2000–1850 emissions. Note difference scales from Fig. 3. **a** Change in aerosol optical depth (AEROD), **b** change in top of atmosphere (TOA) radiation, **c** direct effect of aerosols, **d** change in cloud radiative effect (CRE) or indirect effect of aerosols

clear sky aerosols, but results are similar. We have performed a 50 year free running simulation of the model (internally calculated meteorology with the same boundary conditions), and get nearly identical values (Table 1). ModelE2 has similar global forcing ($-1.1\,\mathrm{Wm}^{-2}$), but with a different separation between direct ($-0.49\,\mathrm{Wm}^{-2}$) and indirect ($-0.60\,\mathrm{Wm}^{-2}$) effects. ModelE2 estimates ACI as a residual of dF−dFdir. Direct effects much larger than in CESM, and concentrated in Europe and E. N. America (Fig. 4c). Indirect effects in ModelE2 are about half that

Table 1 Radiative forcing from different simulations (Wm^{-2})

Simulation	dF	dFdir	ACI(res)	ACI(Δcre)	ΔLWCRE	ΔSWCRE
CESM						
Free 2000–1850	−1.393	−0.045		−1.180	0.557	−1.737
SD 2000–1850	−1.419	−0.068		−1.206	0.482	−1.688
SD 2000–1980	−0.264	−0.025		−0.163	0.075	−0.238
SD 2005–2000	−0.027	0.001		−0.020	0.001	−0.020
SD 2010–2000	0.045	0.012		0.032	0.011	0.022
SD 2010A–2000	0.031	0.006		0.024	0.065	−0.041
SD 2010A2–2000	0.055	0.021		0.027	0.049	−0.022
Model E2						
2000–1850	−1.10	−0.49	−0.60			
2010A2–2000	−0.003	0.05	−0.05			
2010RCP–2000	−0.01	0.04	−0.05			

dF is the change in net top of atmosphere (TOA) flux between simulations, dFdir is the direct effect of aerosols. ACI (res) is ACI estimated at the residual of dF–dFdir for ModelE2. ACI(Δcre) is the indirect effect estimated from the cloud radiative effect (CRE) change in CESM. ΔLWCRE and ΔSWCRE are the long wave (LW) and shortwave (SW) CRE changes

in CESM, for a similar global net total. The reason for the differences for direct effects are likely due to aerosol treatments (such as Nitrate) and are consistent with the analysis of Shindell (2014). The indirect effect treatments are also different, in that ModelE2 includes only the effect on drop number, and not potential lifetime effects. Thus it would seem these lifetime and feedback effects in CESM would be significant.

Table 1 also shows a series of CESM SD runs showing the differences between 2000 and 1980, 2005 and 2000. Since emission changes get smaller with shorter time intervals, the radiative forcing drops significantly, from a total TOA change of −1.4 (from 1850) to −0.26 (from 1980), to −0.03 (between 2005 and 2000). ACI drop accordingly.

Finally, Table 1 illustrates changes between 2010 and 2000. Three different approaches to defining the sulfate emissions have been explored as discussed in Sect. 2.3. The standard case scales uniformly, the 'A' case scales with a threshold ratio to control regions with small changes and 'A2' cases scale by sectors and a threshold. Each simulation has similar global average dF change from 2000 to 2010, in the range of 0.03–0.06. These values are actually slightly positive: so in the opposite sense of a 'hiatus' in warming. Note that there was net radiative cooling (negative forcing) between 2000 and 2005, with subsequent net radiative warming to 2010.

ModelE2 also has very small changes, with a similar positive change in the direct effects, but a negative change (cooling) in the indirect effects. The opposite sign is possible due to the changing nature of emissions locations in the recent period, and the fact that indirect effects are more sensitive in low emission (clean) regions than in high emission (polluted) regions. If emissions increase in regions with lower emissions (Asia), the initial change in indirect forcing is large, but not direct forcing. While if emissions decrease in regions of large emissions (N. America, Europe), there may be few reductions in indirect effects, but significant changes in direct effects. As a consequence of this pattern change and partial cancellation, it is not possible to estimate a forcing efficiency.

The pattern of forcing between 2010 and 2000 is shown in Fig. 5 from CESM and Fig. 6 from ModelE2. Note that the scales are different between Figs. 3 and 5, by a factor of 3 for aerosol optical depth (Fig. 5a) and a factor of 7.5 for the radiative forcing (Fig. 5b–d). Also note that the AOD scale is different for ModelE2 in Fig. 6a, but panels B–D have the same scale in Figs. 5 and 6. As in Fig. 3, the 95 % significance level is for differences larger than about $0.4\,Wm^{-2}$, so the colored regions are statistically significant. Compared to the 2000–1850 differences, a different picture emerges. There is negative forcing (cooling) in the N. Pacific and S. E. Asia due to the increases in SO_2 emissions (Fig. 2d) and AEROD (Fig. 5a) in India and China. There are decreases in AEROD and positive forcing (warming) over N. America and Europe however. As with the case for 1850, the changes in CESM are mostly due to ACI (indirect) effects of changes in cloud radiative effect (Fig. 5d) not direct effects (Fig. 5c). Figure 6 illustrates forcing from ModelE2. Because the dynamics are not specified, the noise level in ModelE2 is higher, but the patterns of positive forcing (warming) over N. America and Europe, and negative forcing (cooling) over the N. Pacific are consistent between simulations. The magnitudes are also similar: more so than for 2000–1850 changes. Model E2 has significant forcing over the Indian Ocean (Fig. 6b) while CESM does not (Fig. 5b). While the global values in Table 1 are small and may not be statistically significant, we will demonstrate that the patterns result in coherent temperature changes.

3.2 Surface temperature

In addition to specified dynamics simulations, we also perform slab ocean model simulations with CESM and an

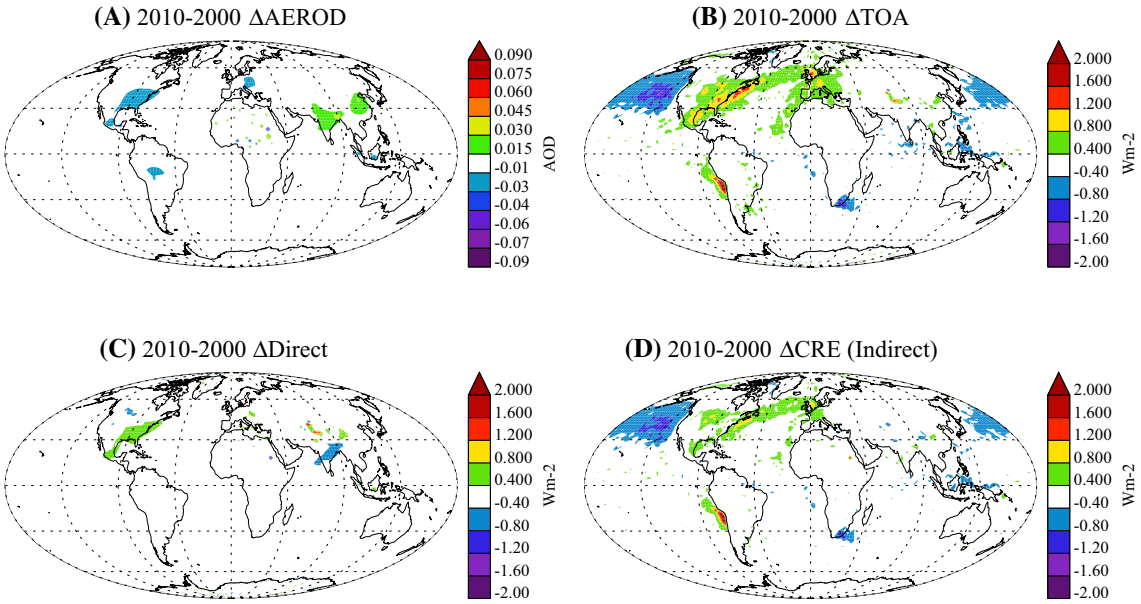

Fig. 5 Radiative forcing from CESM specified dynamics simulations based on 2010–2000 emissions. **a** Change in aerosol optical depth (AEROD), **b** change in top of atmosphere (TOA) radiation, **c** direct effect of aerosols, **d** change in cloud radiative effect (CRE) or indirect effect of aerosols. Note difference scales from Fig. 3

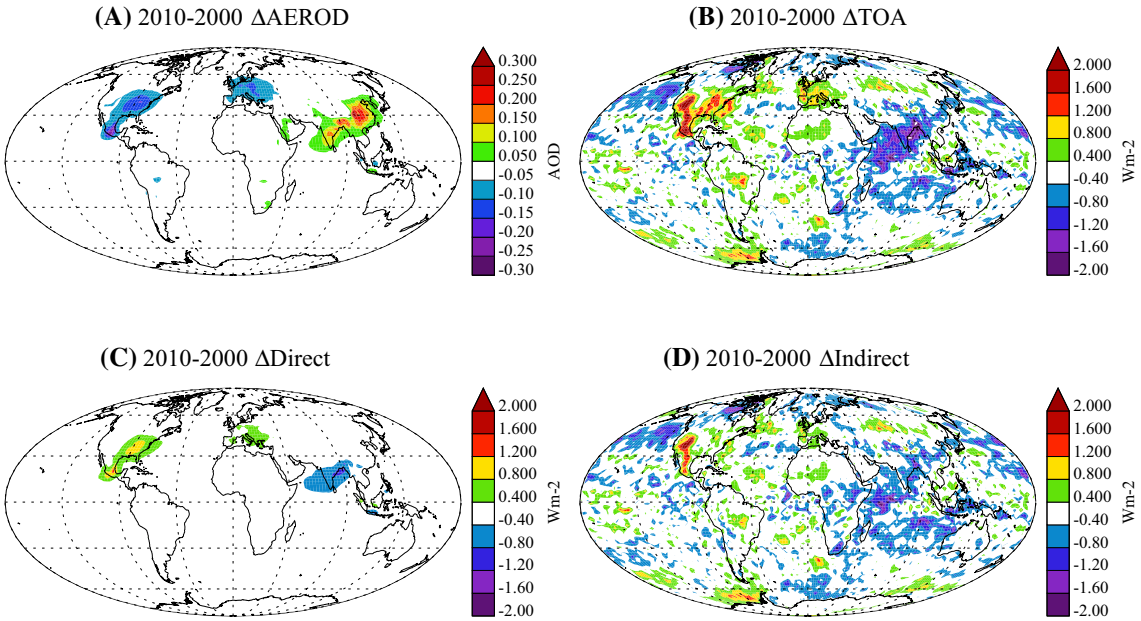

Fig. 6 Radiative forcing from ModelE2 simulations based on 2010–2000 emissions. **a** Change in aerosol optical depth (AEROD), **b** change in top of atmosphere (TOA) radiation, **c** direct effect of aerosols, **d** change in cloud radiative effect (CRE) or indirect effect of aerosols

ensemble of fully coupled simulations with ModelE2 to explore the impact on temperatures. Table 2 illustrates the surface temperature (T_s) impact of the radiative forcing. For aerosol emissions increases (from 1850 or 1980 to 2000) the planet cools, and most of the cooling occurs in the N. Hemisphere. For the recent period there is a slight warming in CESM, spread more evenly between hemispheres. ModelE2 has a slight cooling. The values for regions or the globe are not statistically different than zero (based on the variability of annual mean surface temperature). 2005–2000 differences are also not significant, and generally near 0.01 K.

Table 2 Surface temperature changes from different CESM slab ocean simulations and ModelE2 coupled simulations (K)

Simulation	Global ΔT_s	Tropics ΔT_s	N. Hem ΔT_s	S. Hem ΔT_s	γ_a
CESM					
2000–1850	−1.18	−0.92	−1.92	−0.72	0.83
2000–1980	−0.24	−0.19	−0.44	−0.10	0.91
2005–2000	−0.007	−0.01	−0.02	0.01	
2010–2000	0.04	0.03	0.05	0.05	0.89
ModelE2					
2000–1850	−0.30	−0.32	−0.36	−0.19	0.27
2000–1980	−0.031	−0.12	−0.02	0.07	
2010–2000	−0.027	−0.06	−.07	0.04	

Tropics is 20S–20N, N. Hem and S. Hem are the corresponding extratropical regions (20–90 or −90 to −20). Last column is the aerosol sensitivity, γ_a in $KW^{-1}m^2$

Table 3 Aerosol sensitivity, γ_a, or dTs/dF estimated using analysis from Shindell (2014) as described in the text

Simulation	γ_a
CanESM2	0.77
CSIRO-Mk3-6-0	0.57
GFDL-CM3	1.03
HadGEM2	0.88
IPSL-CM5A-LR	1.52
MIROC, MRI, Nor AVG	0.64

The forcing (Wm^{-2}: Table 1) and response (K: Table 2) can be used to look at the sensitivity of global surface temperature to aerosol forcing where the "aerosol sensitivity" is defined as $\gamma_a = \Delta T_s/\Delta F$. This is analogous to a "climate sensitivity" but for aerosols. It need not be constant with forcing, but Table 2 indicates it is rather constant for CESM and of the same sign as forcing varies over a wide range. Small changes in ΔF (2005–2000 for CESM, and 2000–1980 as well as 2010–2000 for ModelE2) do not yield a reasonable ratio. There are big differences between the two models: the sensitivity of CESM is three times that of ModelE2 for the larger 2000–1850 changes in aerosol.

How representative are these aerosol sensitivities? An approximate estimate of γ_a can be derived from the analysis of CMIP5 models by Shindell (2014). Shindell (2014) estimated the transient climate response to doubled CO_2 for the inhomogeneous forcing agents using two methods (either estimating that stratospheric water acted like a WMGHG and land-use forcing behaved like aerosols+ozone or that land use basically canceled out stratospheric water). Averaging those two methods together, then multiplying by the dF($2xCO_2$) forcing in each model to convert from dTs/dF($2xCO_2$ + Aero) to dTs/dF_a (γ_a) yields the results in Table 3.

The estimates in Table 3 are really for aerosols+ozone in several models, and there are uncertainties due to the limited land use forcing information (though those seem small given the similarity in the results using the two methods), so the comparison is imperfect. Nonetheless, there is a large range from 0.57 to 1.52. The values of γ_a for CESM are in the middle of the range, and for ModelE2 are below the range. ModelE2 is lower than other models, which may be due to a different balance of direct and indirect effects with different vertical structures to their radiative effects. For our purposes though, it is useful to have two models which have a wide range of aerosol sensitivity.

Note that CESM uses a slab ocean, while ModelE2 uses a full dynamic ocean. The difference may induce differences in response to forcing as noted earlier. But based on previous work with CESM slab v. full ocean configurations by Bitz et al. (2012) and Shell (2013), the systematic uncertainties in response between a slab and full ocean are likely to be only a small portion of the differences in response seen here, especially for small perturbations from the control state that would not alter 'equilibrium' oceanic heat uptake (which is specified from a coupled CESM simulation).

The patterns of surface temperature changes resulting from aerosol forcing are illustrated in Fig. 7 for CESM. The significance level for annual mean surface temperature differences at any location over 50 years of CESM slab ocean simulation is about 0.1–0.2 K, based on 90 % confidence of a two sided T test. Thus most of the recent changes in CESM are significant, with the exception of most of the S. Hemisphere in Fig. 7b and the S. H. Oceans in Fig. 7c (the first contour at about 0.15 K). N. Hemisphere cooling is clearly evident in CESM from 1850 (Fig. 7a) and 1980 (Fig. 7b), and is significant in most places. There is cooling over Central Asia, and high latitudes of E. Canada. There are moderate changes in Europe, and even a bit of warming between 1980 and 2000 (Fig. 7b). Throughout, changes in the S. Hemisphere are small. Note the scales are also changing between the panels. There is very little global mean change between 2010 and 2000 (Fig. 7c), but some defined patterns: warming over Central Asia, and cooling in the N. Pacific and W. Pacific. There are some S. Hemisphere changes at high latitudes, and changes in the sub-tropical S. E. Pacific ocean off the coast of S. America. These regions are statistically significant.

CESM experiments are done with a slab ocean. We have also performed similar experiments with a different framework in ModelE2: an ensemble of simulations with RCP4.5 aerosols were compared, and temperature differences of 2012–2008 v. 1995–2005 analyzed. These differences mostly pass a similar 90 % significance test. Note that consistent with lower aerosol sensitivity, the temperature scales have been reduced in Fig. 8. As with CESM, there

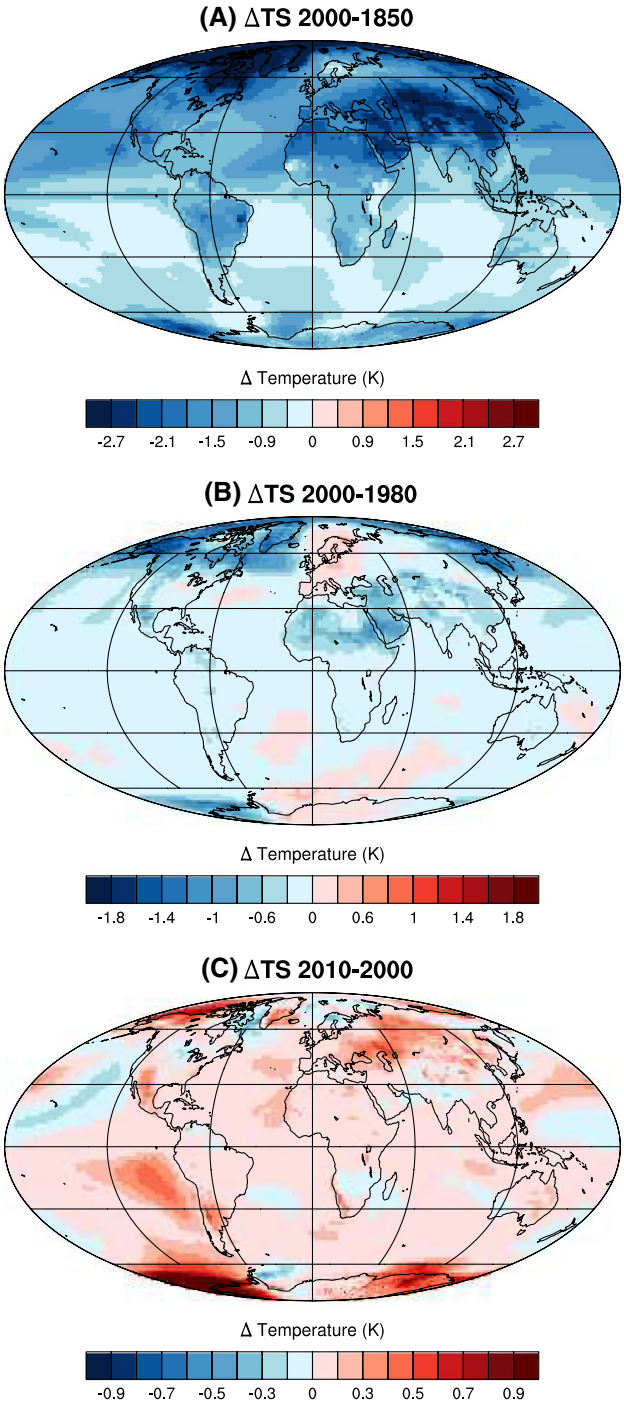

Fig. 7 Maps of CESM simulated surface temperature changes from slab ocean model experiments with aerosol emissions from different years (1850, 1980, 2000, 2010): **a** 2000–1850, **b** 2000–1980, **c** 2010–2000

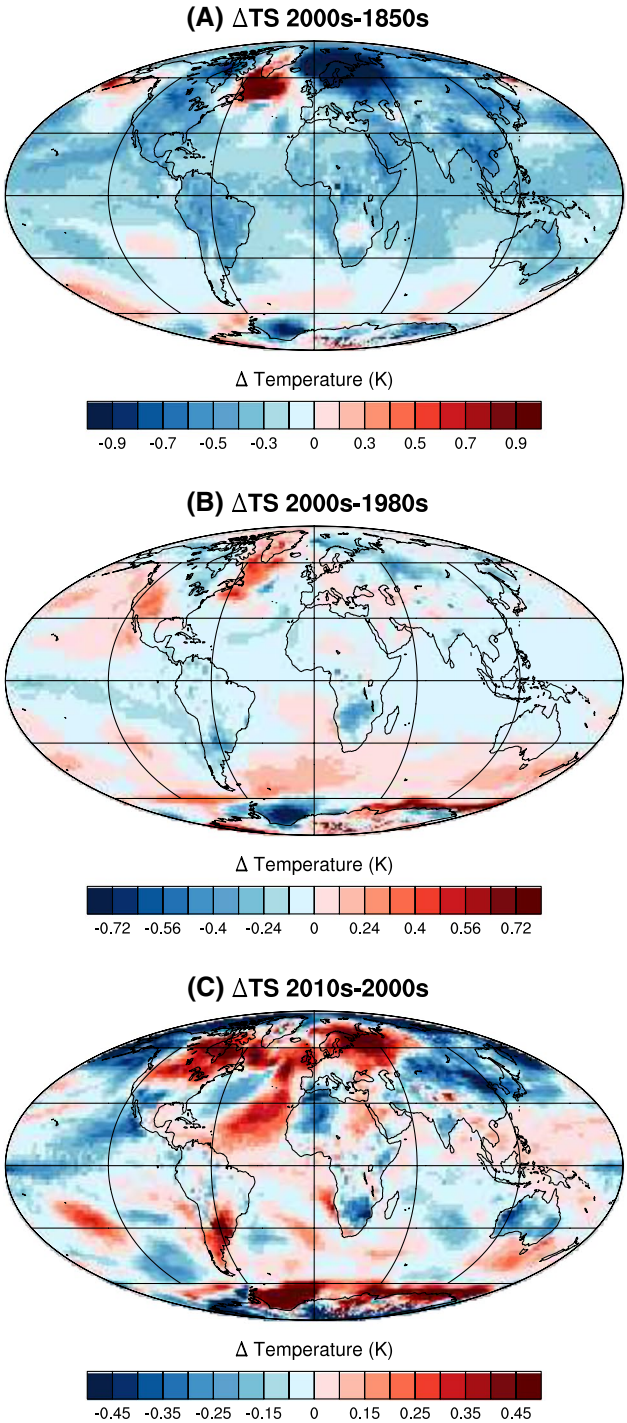

Fig. 8 Simulated ModelE2 surface temperature changes from coupled model experiments with aerosol emissions from different years (1850, 1980, 2000, 2010): **a** 2000–1850, **b** 2000–1980, **c** 2010–2000

is significant cooling from 2000 to 1850 aerosol emissions changes (Fig. 8a). From 2000 to 1980 (Fig. 8b) there is less cooling than CESM. Over the recent period (Fig. 8c) patterns of temperature change from ModelE2 are also similar to CESM: with warming over Europe and E. Canada, and cooling in the N. W. Pacific and over Asia.

How do these changes compare to observations for the recent past? The global magnitude of forcing over

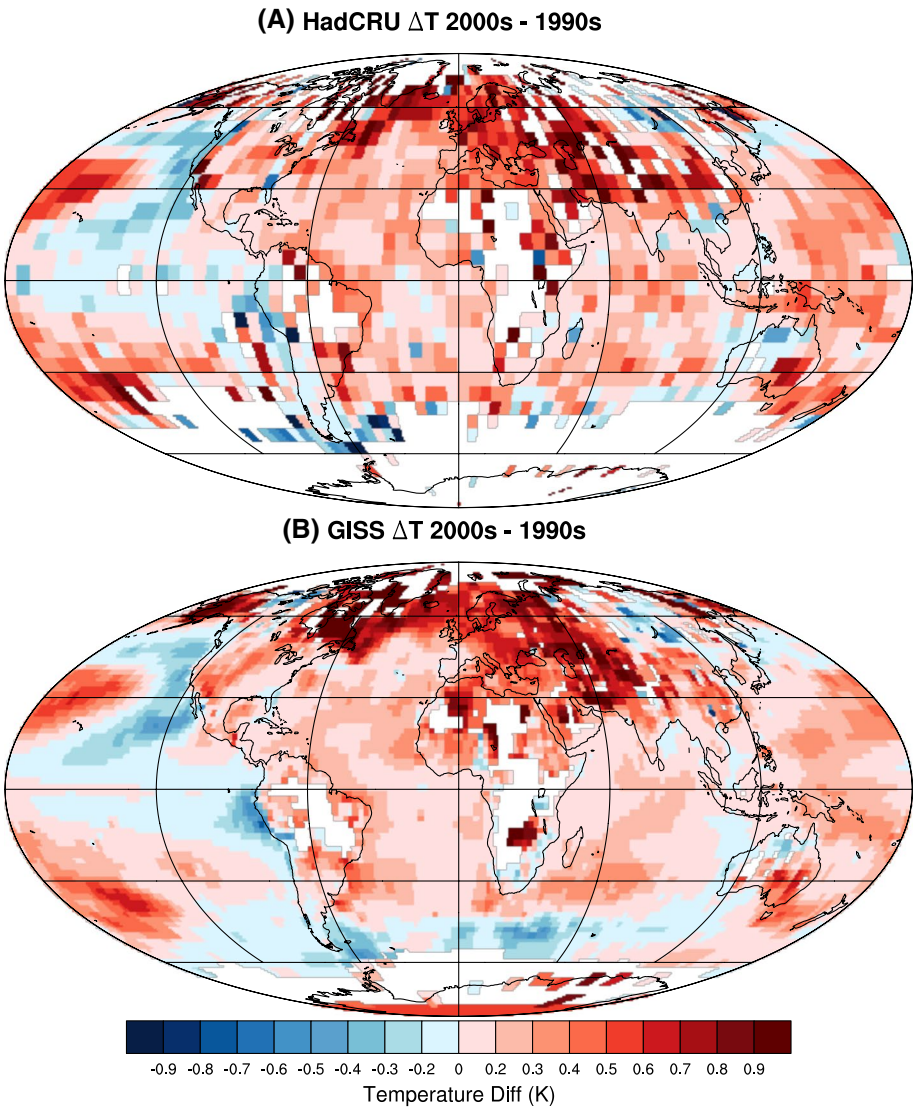

Fig. 9 Observed Decadal surface temperature differences: 2000s (2001–2011) 1990s (1990–1999). **a** HadCRUT3, **b** GISS. ENSO anomalies removed

2010–2000 is small, and not different from zero (Table 1), but the pattern of forcing and response is similar in models, despite different aerosol forcing and sensitivity. To compare to observations of surface temperature, we use decadal averages of temperature from the 1990s (1990–1989) and the most recent decade (2001–2011), and difference these two decades in Fig. 9 from both the (A) HadCRUT3 and (B) GISS temperature records. Decadal anomalies are very similar with HadCRUT4 data (not shown), but with extrapolation to the Arctic. Because internal modes of variability, particularly the El Niño Southern Oscillation (ENSO) can have large effects on tropical and global temperatures (Schmidt et al. 2014a; Kosaka and Xie 2013), we remove these effects. ENSO is removed by regressing monthly temperature anomalies at each point on the Nino3.4 SST anomalies (5°S–5°N and 170–120°W), and then removing the regression coefficient (at every point) times the Nino3.4 index (for each month). Mostly the regression just affects the equatorial Pacific: there is larger cooling without ENSO removed, due to the enhanced ENSO events in the 1990s. The patterns are similar between the data sets, with recent warming over Europe and E. Canada, and some cooling in the S. Hemisphere and in the Pacific.

The major temperature differences in the recent 'hiatus' period in Fig. 9 has some features in common (cooler N. Pacific, warmer Atlantic and Europe) with the simulated temperature response to aerosol forcing in Figs. 7 and 8. To quantitatively compare to simulations, we use the GISS T_s data (since it has more complete coverage) with ENSO removed (Fig. 9b), and compare to the 2010–2000 CESM simulation (Fig. 7c) on the same scale in Fig. 10. By eye, there are quite a few similarities between the patterns: including cooling in the N. E. Pacific, and warming over Europe, with some cooling in the S. Hemisphere at different latitudes. To quantify these similarities, uncentered pattern correlations are performed. Uncentered global pattern

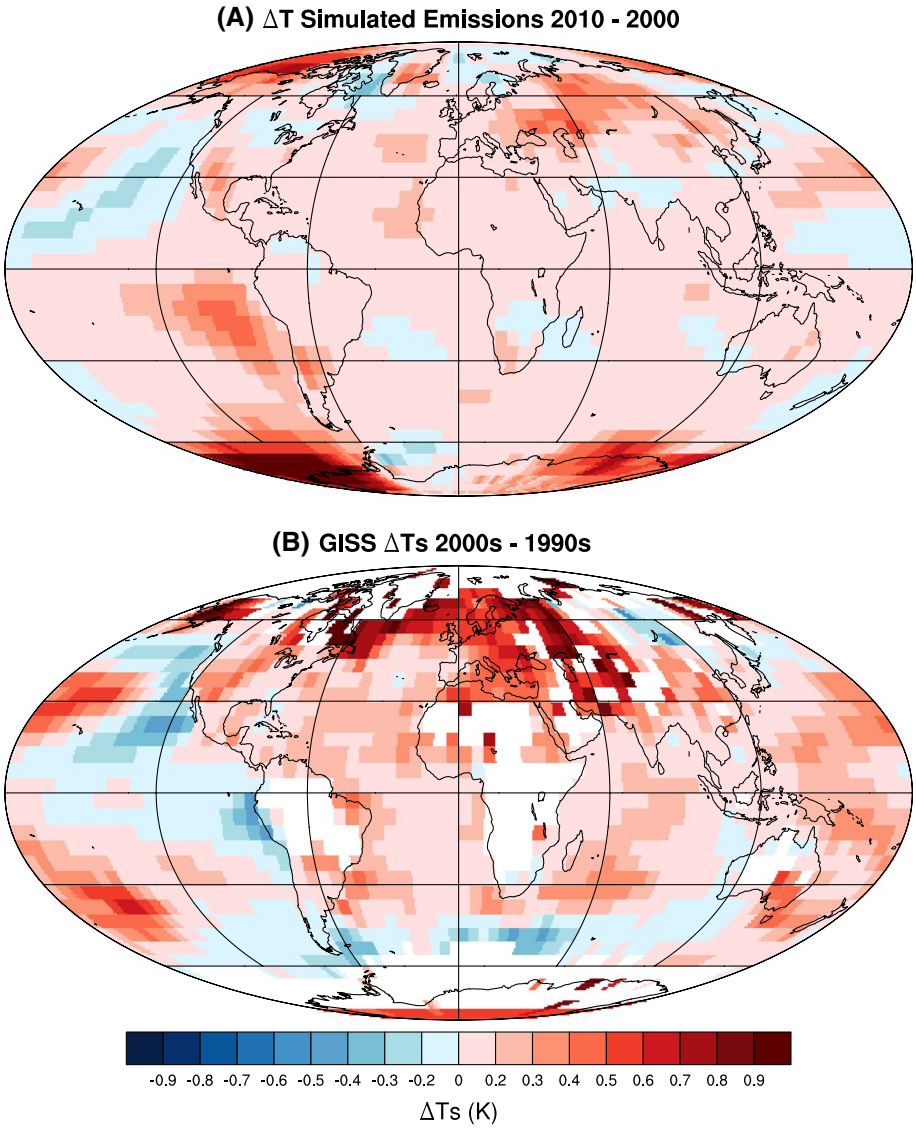

Fig. 10 Decadal surface temperature differences. **a** Simulated with slab ocean experiments 2010–2000 emissions. **b** Observed GISS surface temperature differences: 2000s (2001–2011) 1990s (1990–1999) ENSO anomalies removed

correlations between the CESM simulated (2010–2000) surface temperature differences and the observed decadal (2000s–1990s) surface temperature differences are 0.43 with GISS T_s and 0.35 with HadCRUT3 T_s (0.34 with HadCRUT4 T_s). The pattern correlation between GISS and HadCRUT3 data sets is 0.82, giving some indication of the variability of the metrics and what might be expected. These are significant correlations at the 95 % level based on a 2-sided Student's T test, using a small number of degrees of freedom (36: one for each regridded latitude). Correlations are slightly higher in the N. Hemisphere (0.46) than over the S. Hemisphere (0.23). Seasonal correlations show the strongest pattern correlations in the Northern hemisphere in June–August (0.25 HadCRUT3, 0.32 GISS) and September-November (0.44 HadCRUT3, 0.47 GISS). This would be consistent with large impacts of the forcing on higher short wave cloud radiative effects in the summer season and extending into fall. There is little consistent seasonality of pattern correlations in the S. Hemisphere. Seasonal correlations are often lower than the annual mean because of higher internal variability on smaller temporal scales.

We have also examined pattern correlations with the ModelE2 simulations, but as these are short coupled simulations, they are not expected to be in full equilibrium. However, they do represent a transient simulation, and provide a further idea of whether we can expect a signal. The fully coupled ModelE2 simulations have warming over N. American and Europe, cooling over Asia and the Pacific in Fig. 8c. This is similar to CESM and to observed decadal differences. Pattern correlations are 0.08 Global and 0.15 in the Northern Hemisphere with no correlation in Southern Hemisphere. The ModelE2 pattern correlations are statistically significant at the 90 % level assuming 1 degree

of freedom for each hemisphere, each year. Thus similar response patterns are seen in coupled simulations.

4 Conclusions

We have explored the radiative forcing resulted from recent changes to anthropogenic emissions of SO_2 (holding other forcing agents constant) in two Earth System Models with different sensitivity to aerosols (γ_a). There are similar patterns and magnitudes to the resulting radiative forcing. There are regions of negative and positive forcing offsetting each other in the global mean. Negative forcing results due to increases of emissions in S. Asia and E. Asia, which cools those regions and the N. Pacific. Positive forcing occurs with decreases in aerosol emissions and loading in N. America and Europe, yielding reductions in aerosol effects (a warming) over the recent decade over a broad region from N. America through the Atlantic to N. Europe. Both CESM and ModelE2 show this. The forcing pattern is consistent with AOD changes. Most of the TOA changes are indirect effects of aerosols (ACI). The net global effects of aerosols over the period are almost zero as a result of these offsetting patterns. We do not find that aerosols exerted a significant global negative forcing over the last decade or so. This is different than hypothesized by Schmidt et al (2014a, b). But here we neglect possible effects of NO_2 and NH_3 from nitrate aerosols, which may under-represent ACI as a result.

The 'hiatus', or lack of recent warming in surface temperature is mostly a northern hemisphere effect, with small trends in the global mean. If the 'hiatus' is a data artifact [Cowtan and Way (2014) and red line in Fig. 1], then a minimal response to aerosol forcing at the global scale during recent decades may also be consistent with global mean temperature trends as well as regional trends.

The new emissions scenarios estimate increases in emissions to 2005, and then some decreases, largely due to emissions controls in China (Lu et al. 2010). This has partially reversed the global impact of SO_2 increases on ACI, combined with continuing decreases in SO_2 from Europe and N. America) There are however possibly large changes over the (relatively clean) oceans due to increases in bunker fuels from ships. In the simulations this results in significant regional forcing over the N. E. Pacific.

Different techniques were used to try to elucidate the surface temperature climate response in CESM and ModelE2. We explored the impacts of aerosols using the RCP emissions (in ModelE2) and an alternative estimate of SO_2 emissions (in CESM), but that certainly doesn't span either the full range of possible aerosol-related emissions or the full range of uncertainties in representing aerosol physics in the models. However, the models have very different aerosol sensitivities (γ_a), and we get similar results, indicating that there are some robust responses.

There are some common temperature patterns between observed decadal changes over the last 10 years and the simulated responses: warming in the Atlantic and cooling in the Pacific. These patterns are consistent with the radiative forcing from recent aerosols, with significant pattern correlations in CESM and ModelE2 in the Northern Hemisphere. Pattern correlations are lower in the full coupled simulations with ModelE2. Aerosols may be contributing to the regional pattern of forcing, but do not appear be the dominant factor leading to the 'hiatus' in warming (if it exists). It is possible that the aerosol forcing pattern may force modes of variability in the earth system, such as forcing in the North Atlantic that may alter the meridional overturning circulation for example, which we do not capture in the slab ocean (CESM) or short coupled (ModelE2) simulations. We have considered the major effect of aerosols on clouds through sulfate, but other responses (e.g., from nitrate) that are neglected here are possible. Pattern correlations are suggestive that there is an aerosol imprint on the temperature response. With the internal variability and the strength of the aerosol-induced response in these two models it's extremely difficult to detect the influence of aerosols over this time period.

The overall magnitude of the changes in forcing from the two models indicates that ACI contributions from sulfate are a near zero global forcing agent over the last decade of less than $\pm 0.1\ \mathrm{Wm}^{-2}$. This compares to a positive anthropogenic greenhouse gas forcing of $+0.35\ \mathrm{Wm}^{-2}$. Other agents can easily account for this, including oceans heat uptake ($-0.2\ \mathrm{Wm}^{-2}$, Trenberth et al. (2014)), stratospheric water vapor decreases ($-0.1\ \mathrm{Wm}^{-2}$, Solomon et al. (2010)), recent volcanoes ($-0.1\ \mathrm{Wm}^{-2}$, Solomon et al. (2011)), and effects from variations in solar flux over the 11 year solar cycle and ENSO variability (Kosaka and Xie 2013).

What does this mean for the future? Variability in ocean heat uptake is likely to continue to play a large role. None of these negative forcings will continue forever (many are transient), and aerosols are now decreasing. At some point continued increases in anthropogenic greenhouse gas forcing, if growth rates remain the same, will overwhelm other forcings on and variability of the climate system. Transient forcings are likely to revert to a mean, most likely resulting in future return to increases in global mean temperature.

Acknowledgments The National Center for Atmospheric Research is sponsored by the U.S. National Science Foundation. Thanks to S. Tilmes and P. Bogenschutz for comments, and Greg Faluvegi for assistance with ModelE2 simulations. CESM Computing resources (ark:/85065/d7wd3xhc) were provided by the Climate Simulation Laboratory at NCAR's Computational and Information Systems Laboratory, sponsored by the National Science Foundation and other agencies. ModelE2 computer resources were provided by the NASA

High-End Computing Program through the NASA Center for Climate Simulation at Goddard Space Flight Center.

References

Albrecht BA (1989) Aerosols, cloud microphysics and fractional cloudiness. Science 245:1227–1230

Bitz C, Shell KM, Gent PR, Bailey D, Danabasoglu G, Armour KC, Holland MM, Kiehl JT (2012) Climate sensitivity of the Community Climate System Model version 4. J Clim 25:3053–3070. doi:10.1175/JCLI-D-11-00290.1

Booth BB, Dunstone NJ, Halloran PR, Andrews T, Bellouin N (2012) Aerosols implicated as a prime driver of twentieth-century north atlantic climate variability. Nature 484(7393):228–232. doi:10.1038/nature10946

Boucher O, Randall D, Artaxo P, Bretherton C, Feingold G, Forster P, Kerminen VM, Kondo Y, Liao H, Lohmann U, Rasch P, Satheesh S, Sherwood S, Stevens B, Zhang X (2013) Clouds and aerosols. In: Stocker TF, Qin D, Plattner GK, Tignor M, Allen S, Boschung J, Nauels A, Xia Y, Bex V, Midgley P (eds) Climate change 2013: the physical science basis. Contribution of working group I to the fifth assessment report of the intergovernmental panel on climate change, chapter 7. Cambridge Universtiy Press, Cambridge

Brohan P, Kennedy JJ, Harris I, Tett SF, Jones PD (2006) Uncertainty estimates in regional and global observed temperature changes: a new data set from 1850. J Geophys Res 111(D12106). doi:10.1029/2005JD006548

Chen X, Tung KK (2014) Varying planetary heat sink led to global-warming slowdown and acceleration. Science 345(6199):897–903. doi:10.1126/science.1254937

Cowtan K, Way RG (2014) Coverage bias in the HadCRUT4 temperature series and its impact on recent temperature trends. Q J R Meteorol Soc. doi:10.1002/qj.2297

Gettelman A, Liu X, Ghan SJ, Morrison H, Park S, Conley AJ, Klein S, Boyle J, Mitchell DL, Li JLF (2010) Global simulations of ice nucleation and ice supersaturation with an improved cloud scheme in the Community Atmosphere Model. J Geophys Res 115(D18216). doi:10.1029/2009JD013797

Ghan S (2013) Technical note: estimating aerosol effects on cloud radiative forcing. Atmos Chem Phys 13(19):9971–9974

Hansen J, Ruedy R, Sato M, Lo K (2010) Global surface temperature change. Rev Geophys 48(RG4004). doi:10.1029/2010RG000345

Hartmann DL, Tank AK, Rusticucci M, Alexander L, Brinnimann S, Charabi Y, Dentener F, Dlugokencky E, Easterling D, Kaplan A, Soden B, Thorne P, Wild M, Zhai P (2013) Observations: atmosphere and surface. In: Stocker TF, Qin D, Plattner GK, Tignor M, Allen S, Boschung J, Nauels A, Xia Y, Bex V, Midgley P (eds) Climate change 2013: the physical science basis. Contribution of working group I to the fifth assessment report of the intergovernmental panel on climate change, chapter 2. Cambridge Universtiy Press, Cambridge

Hurrell JW, Holland M, Gent P, Ghan S, Kay JE, Kushner P, Lamarque JF, Large W, Lawrence D, Lindsay K et al (2013) The Community Earth System Model: a framework for collaborative research. Bull Am Meteorol Soc 94(9):13391360. doi:10.1175/BAMS-D-12-00121.1

Kaufmann RK, Kauppi H, Mann ML, Stock JH (2011) Reconciling anthropogenic climate change with observed temperature 1998–2008. Proc Nat Acad Sci 108(29):11790–11793. doi:10.1073/pnas.1102467108

Klimont Z, Smith SJ, Cofala J (2013) The last decade of global anthropogenic sulfur dioxide: 2000–2011 emissions. Env Res Lett 8(014003). doi:10.1088/1748-9326/8/1/014003

Koch D, Bond T, Streets D, Bell N, van der Werf GR (2007) Global impacts of aerosols from particular source regions and sectors. J Geophys Res 112(D02205). doi:10.1029/2005JD007024

Kosaka Y, Xie SP (2013) Recent global-warming hiatus tied to equatorial pacific surface cooling. Nature 501(7467):403–407. doi:10.1038/nature12534

Lamarque JF, Bond TC, Eyring V, Granier C, Heil A, Klimont Z, Lee D, Liousse C, Mieville A, Owen B, Schultz MG, Shindell D, Smith SJ, Stehfest E, Van Aardenne J, Cooper OR, Kainuma M, Mahowald N, McConnell JR, Naik V, Riahi K, van Vuuren DP (2010) Historical (1850–2000) gridded anthropogenic and biomass burning emissions of reactive gases and aerosols: methodology and application. Atmos Chem Phys 10(15):7017–7039. doi:10.5194/acp-10-7017-2010

Lamarque JF, Emmons L, Hess P, Kinnison DE, Tilmes S, Vitt F, Heald C, Holland EA, Lauritzen P, Neu J et al (2012) CAM-chem: description and evaluation of interactive atmospheric chemistry in the Community Earth System Model. Geosci Model Dev 5:369–411

Lean JL, Rind DH (2009) How will earth's surface temperature change in future decades? Geophys Res Lett 36(L15708). doi:10.1029/2009GL038932

Liu X et al (2012) Towards a minimal representation of aerosol direct and indirect effects: model description and evaluation. Geosci Model Dev 5:709–735. doi:10.5194/gmd-4-709-2012

Lu Z, Streets D, Zhang Q, Wang S, Carmichael G, Cheng Y, Wei C, Chin M, Diehl T, Tan Q (2010) Sulfur dioxide emissions in China and sulfur trends in East Asia since 2000. Atmos Chem Phys 10(13):6311–6331. doi:10.5194/acp-10-6311-2010

Menon S, Koch D, Beig G, Sahu S, Fasullo J, Orlikowski D (2010) Black carbon aerosols and the third polar ice cap. Atmos Chem Phys 10:4559–4571. doi:10.5194/acp-10-4559-2010

Miller RL et al (2014) CMIP5 historical simulations (1850–2012) with GISS ModelE2. J Adv Model Earth Syst 6:441–477. doi:10.1002/2013MS000266

Morrison H, Gettelman A (2008) A new two-moment bulk stratiform cloud microphysics scheme in the NCAR Community Atmosphere Model (CAM3), part I: description and numerical tests. J Clim 21(15):3642–3659

Neale RB, Chen CC, Gettelman A, Lauritzen PH, Park S, Williamson DL, Conley AJ, Garcia R, Kinnison D, Lamarque JF, Marsh D, Mills M, Smith AK, Tilmes S, Vitt F, Cameron-Smith P, Collins WD, Iacono MJ, Easter RC, Ghan SJ, Liu X, Rasch PJ, Taylor MA (2010) Description of the NCAR Community Atmosphere Model (CAM5.0). In: Technical report NCAR/TN-486+STR. National Center for Atmospheric Research, Boulder

Schmidt GA, Shindell DT, Tsigaridis K (2014a) Reconciling warming trends. Nat Geosci 7(3):158–160

Schmidt GA et al (2014b) Configuration and assessment of the GISS ModelE2 contributions to the CMIP5 archive. J Adv Model Earth Syst 6:141–184. doi:10.1002/2013MS000265

Shell KM (2013) Consistent differences in climate feedbacks between atmosphereocean GCMs and atmospheric GCMs with slab-ocean models. J Clim 26:42644281. doi:10.1175/JCLI-D-12-00519.1

Shindell DT (2014) Inhomogeneous forcing and transient climate sensitivity. Nat Clim Change 4:274–277

Solomon S, Rosenlof KH, Portmann RW, Daniel JS, Davis SM, Sanford TJ, Plattner GK (2010) Contributions of stratospheric water vapor to decadal changes in the rate of global warming. Science 327(5970):1219–1223. doi:10.1126/science.1182488

Solomon S, Daniel JS, Neely RR, Vernier JP, Dutton EG, Thomason LW (2011) The persistently variable "background" stratospheric

aerosol layer and global climate change. Science 333(6044):866–870. doi:10.1126/science.1206027

Taylor KE, Stouffer RJ, Meehl GA (2012) An overview of CMIP5 and the experimental design. Bull Am Meteorol Soc 93:485–498. doi:10.1175/BAMS-D-11-00094.1

Trenberth KE, Fasullo JT, Balmaseda M (2014) Earth's energy imbalance. J Clim 27:3129–3144. doi:10.1175/JCLI-D-13-00294.1

Twomey S (1977) The influence of pollution on the shortwave albedo of clouds. J Atmos Sci 34(7):1149–1152